Polyamine-Guided Synthesis of Anisotropic, Multicompartment Microparticles

Vinit S. Murthy,[†,‡] Shyam B. Kadali,[†,§,‖] and Michael S. Wong*[,†,§]

Departments of Chemical and Biomolecular Engineering and of Chemistry, Rice University, 6100 S. Main Street, Houston, Texas 77251-1892

ABSTRACT Colloidal particles that have nonuniform bulk or surface compositions are of emerging interest because of their potential applications involving advanced chemical storage and delivery and the self-assembly of novel functional materials. Experimental realization of anisotropic particles is much more difficult than that for particles with uniform bulk and surface composition, however. A new wet-chemical synthesis method to anisotropic microparticles is presented. This approach makes convenient use of the unusual observation of a salt-triggered separation of two water-solubilized polyamines into colloidal aggregates with nonuniform polymer composition. The anisotropic structure of these ionically cross-linked aggregates is explained by the difference in surface tensions of the contained single-polymer domains. Contacting the polymer aggregates with silicic acid or 13-nm silica nanoparticles leads to the charge-driven formation of solid or hollow microspheres, respectively. Depending on the poly(lysine)/poly(allylamine) ratio, the nonuniformity of the polymer aggregates translates to surface patches or internal compartments found in the resultant silica/polymer microparticles. Such hybrid materials with their unique structure could serve as a new basis for targeted chemical delivery and controlled release for potential applications in medicine, food, and cosmetics.

KEYWORDS: assembly • colloidal • hybrid • materials • silica • nanoparticles • polymers • carbon/silicon/oxides

Anisotropic particles are those that have a nonspherical shape, nonhomogeneous surface, nonhomogenous bulk composition, and/or multiple compartments (1, 2). Patchy particles and multicompartment particles are two types that have garnered a great amount of attention in recent years. Both can be prepared using a number of methods, but the preparation approaches are relatively few and are restricted to certain size ranges and compositions.

Independent of size, patchy particles can be defined as those having surface functional groups at prescribed locations, as opposed to the general case of particles with surfaces uniformly covered by functional groups. Such particles have been demonstrated to serve as much more efficient building blocks to create premeditated, higher-order complex architectures owing to their built-in recognition sites that can direct the self-organization of particles (1, 3−8). Suprastructures thus formed have potential use in self-assembling electronic circuits, photonic crystals, biomedical applications, electrorheological fluids, and switching devices (9−12).

Several techniques have been studied to fabricate patchy microparticles (diameter >1000 nm) and submicron-sized particles (or mesoparticles, diameter = 100−1000 nm (13)), such as the Langmuir−Blodgett techniques (10), microcontact printing (12), and physical vapor deposition of metals onto an interface-stabilized colloid monolayer (9, 14−16). These preparation routes require multiple steps to be performed sequentially and yield relatively small amounts of material. An example of patchy nanoparticles (NPs, diameter of 1−100 nm) arising from the angstrom-level self-ordering of two different-length alkylthiols into a rippled surface pattern on Au NP surfaces was reported recently (17).

Whereas patchy particles have a nonuniform surface, multicompartment particles have a nonuniform internal bulk structure because they contain multiple domains within the particle perimeter. Such particles are being sought for advanced chemical storage and controlled release applications in pharmaceuticals, foods, cosmetics, and related industries (2, 18−21). They can be prepared at the micronscale and mesoscale using microfluidic or electrospraying techniques (22−25) and at the nanoscale through the kinetically driven self-assembly of designer triblock copolymers (19, 26, 27).

We present a new and convenient wet-chemical synthesis strategy to anisotropic microspheres that makes use of the unusual observation of phase separation of water-solubilized polyamines into two-polymer colloidal aggregate intermediates. Our synthesis route draws on earlier work on NP/polymer microcapsules via charge-driven tandem assembly of polyamines and NPs (13, 28−33). Cationic polyamines [e.g., poly(L-lysine hydrobromide) (PLL) and poly(allylamine hydrochloride) (PAH)] are brought into contact with multivalent anions (e.g., sodium citrate) under aqueous conditions to form salt-cross-linked polymer aggregates. Negatively charged NPs (e.g., SiO$_2$ NPs) are then added to this suspension of spherical aggregates. The NPs diffuse into the outer

Scheme 1. Model Structures of Silica/Polymer Hollow Spheres That Are (a) Polymer-Filled or (b) Water-Filled and (c) Silica/Polymer Solid Spheres
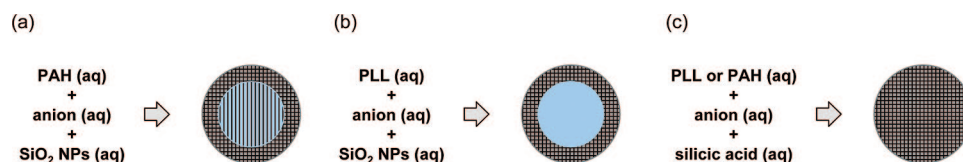
portion of the polymer/salt aggregate and deposit to form a thick shell wall such that the wall contains NPs and polymer (Scheme 1). This diffusion/deposition route to forming capsule shells occurs in one processing step. In contrast, the layer-by-layer assembly of capsules involves the deposition of charged particles or polymers multiple times around a solid or a liquid core template, with the shell thickness controlled by the number of deposition steps (34, 35). Using small enough NPs like those in a silicic acid solution leads to silica/polymer solid spheres because it is thought that these smaller NPs can diffuse completely throughout the polymer/salt aggregate (30).

The thus-formed hollow spheres are based on electrostatic interactions for assembly, similar to those prepared through layer-by-layer assembly (34, 35). Unlike the latter, though, the former can be polymer-filled (meaning the polymer/salt aggregate fills the core) if PAH is the polymer (29) or water-filled (the polymer/salt aggregate disassembles during capsule formation) if PLL is the polymer (Scheme 1) (30). In the layer-by-layer assembly method, hollow capsules are formed after removal of the core template through dissolution or calcination. In this work, we hypothesized that a mixture of PAH and PLL also yields capsules through our tandem assembly route, with PAH filling the core and PAH and PLL both residing within the shell.

EXPERIMENTAL SECTION

Materials. Poly(L-lysine hydrobromide) (195 kDa, ~935 lysine units per molecule, bromide counterion, "PLL"), poly(allylamine hydrochloride) (70 kDa, ~750 allylamine units per molecule, chloride counterion, "PAH"), and tetramethylorthosilicate ("TMOS") were all procured from Sigma-Aldrich and were used without further purification. Trisodium citrate ("cit") was obtained from Sigma-Aldrich. SiO_2 NPs (Snowtex-O, Nissan Chemicals) are available as an aqueous colloidal suspension (20 wt %, pH 3.4, ionic strength $I = 16.9$ mM). The NPs measured 13 ± 3 nm in diameter, according to dynamic light scattering (DLS). The ζ potential of SiO_2 NPs in the original sol condition was calculated from its electrophoretic mobility (-1.4 μm s^{-1} V^{-1} cm) to be -16 mV in Henry's limit. The fluorescent dyes of fluorescein isothiocyanate (FITC) and rhodamine B isothiocyanate (RITC) were procured from Sigma-Aldrich. The polyelectrolyte stock solution and all subsequent diluted precursor solutions were made using deionized water (18.2 MΩ, Barnstead Nanopure Diamond System).

Synthesis. Aqueous mixtures of PLL and PAH were prepared by mixing different volume ratios of PLL (4.5 mg mL^{-1}) and PAH (2 mg mL^{-1}) solutions. In order to prepare a 75% PLL/25% PAH mixture, 37.5 μL of a PLL solution was mixed with 12.5 μL of a PAH solution. The concentrations of precursor polymer solutions were chosen such that a 75/25 mixture indicated that 75% of the positive charges in a solution were coming from PLL and the rest 25% from PAH. All experiments with polyelectrolyte/salt solutions were done at specific charge ratio R, which is

defined as the ratio of the total negative charge of the added salt to the total positive charge of the polymers ($R = [\text{anion}]|z_-|/([\text{PAH}]|z_{+,\text{PAH}}| + [\text{PLL}]|z_{+,\text{PLL}}|)$, where z_- is the negative charge per anion, $z_{+,\text{PAH}}$ is the number of positive charges per PAH chain, and $z_{+,\text{PLL}}$ is the number of positive charges per PLL chain). For all experiments, the R value was arbitrarily chosen as 4 using a 12.0 mM cit salt solution. A typical synthesis protocol consisted of mixing different volume ratios of PLL (precursor concentration of 4.5 mg mL^{-1}) and PAH (precursor concentration of 2 mg mL^{-1}) to give a final volume of 50 μL. To this was added 125 μL of a cit salt solution (12 mM, $R = 4$), and the resulting solution was gently mixed for 10 s using a vortex mixer at "5" speed (on a scale from 1 to 10). The resulting suspension was aged for 30 min under quiescent conditions. After the aging period, the suspension was mixed with 50 μL of a 1 M TMOS/HCl aqueous solution (final pH ~ 3.5) and gently homogenized, resulting in solid microspheres. After further aging for 20 min, the suspension was centrifuged and thoroughly washed with deionized water. In order to synthesize hollow microcapsules, TMOS was replaced with 125 μL of a colloidal suspension of SiO_2 NPs.

Dye Conjugation of PAH. A total of 4 mg of FITC was dissolved in 500 μL of dimethyl sulfoxide (DMSO; 99.8+%, EM Science). A total of 500 mg of PAH was dissolved in 6 mL of deionized water, with the solution pH adjusted to 8.4 using NaOH. The two solutions were combined and stirred for 2 days at room temperature in the dark. The resulting solution was dialyzed against deionized water for 48 h (molecular cutoff of 2000 Da, POR 7 dialysis membrane, Spectrum Laboratories), with the final product dried and recovered in a rotary evaporator. A similar procedure was carried out for the synthesis of PAH-RITC, except that 2 mg of the RITC dye was dissolved in 250 μL of DMSO and 250 mg of PAH was dissolved in 3 mL of deionized water (pH adjusted to 9.5).

Characterization. *Confocal Laser Scanning Microscopy.* Confocal images were captured with a Carl Zeiss LSM 510 inverted microscope equipped with a 100× oil immersion objective (NA = 1.4). Laser excitation wavelengths of 488 nm for FITC ($\lambda_{\text{ex}} = 494.5$ nm; $\lambda_{\text{em}} = 520$ nm) and 543 nm for RITC ($\lambda_{\text{ex}} = 560$ nm; $\lambda_{\text{em}} = 590$ nm) were chosen. Samples were mounted on conventional glass slides and sealed under a coverslip to prevent drying. All samples were freshly prepared 1–2 h prior to imaging.

ζ Potential Analysis. ζ potentials were calculated using phase analysis light scattering, a variation of electrophoretic DLS, from electrophoretic mobility measurements using Henry's equation (i.e., $0.1 \leq \kappa a \leq 100$, where κ is the Debye–Hückel parameter and a is the particle radius). A dip-in (Uzgiris type) electrode system with 4 mL polystyrene cuvettes was used.

Scanning Electron Microscopy (SEM). SEM was carried out on a JEOL 6500 field emission microscope equipped with in-lens thermal field emission electron gun. A secondary electron image was taken at a 15 kV electron beam with a working distance of 10 mm. The microsphere suspension was washed twice with water, loaded on the aluminum stub, and dried before imaging. The sample was sputter-coated with gold for 1 min.
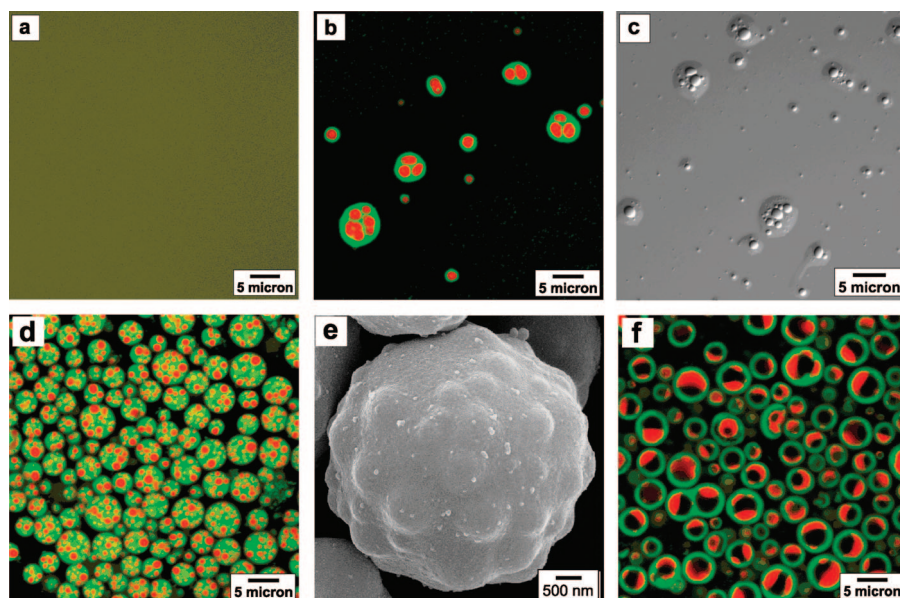
FIGURE 1. Confocal images of (a) an aqueous solution of PLL and PAH (50:50) and (b) the resulting suspension after the addition of a cit solution at $R = 4$, in which fluorescent PLL-FITC and PAH-RITC were used. (c) DIC image of a PLL-PAH/cit aggregate suspension analogous to that shown in part b except that PLL and PAH contained no dye. (d) Confocal and (e) SEM images of solid microspheres after the addition of silicic acid to part b. (f) Confocal image of hollow microspheres after the addition of SiO$_2$ NPs to part b.

Optical Microscopy. Optical microscopy was performed on a Leica DM2500 upright microscope equipped with a 100× oil immersion objective (NA 1.4).

RESULTS AND DISCUSSION

Figure 1a shows a fluorescence overlay image of a mixed aqueous solution of PLL and PAH, with a PLL/PAH ratio of 50:50 (meaning that 50% of the total amine units in solution were from PLL and 50% were from PAH). When the multivalent citrate salt solution was added, the solution immediately turned turbid, indicating the presence of submicron-sized polymer/salt aggregates. Quite intriguingly, these aggregates were composed of distinct PAH domains (colored red) distributed inside larger PLL aggregates (colored green, Figure 1b). Homogeneously mixed in an aqueous solution, PLL and PAH chains underwent a sort of phase separation into globules after contact with the citrate salt; smaller aggregates ($< \sim 2 \, \mu$m) had a PAH-core/PLL-shell structure and larger aggregates ($> \sim 2 \, \mu$m) contained multiple PAH cores.

The charge ratio R is an important synthesis parameter in polymer/salt aggregate formation. No differences in PLL-PAH (50:50)/cit aggregate structures were found across the wide range of R values (2−100), and so all subsequent experiments were performed at $R = 4$.

This citrate-induced phase separation of PLL and PAH has not been reported previously and is unlike other colloidal systems. For comparison, the self-assembled polymer/salt aggregates of Pochan, Wooley, and co-workers come from poly(acrylic acid)/poly(methyl acrylate)/polystyrene triblock copolymers that coassemble with oppositely charged amine organic cations in a tetrahydrofuran/water solution (36−38). The fascinating shapes and internal structuring of these aggregates (with features on the order of tens of nanometers) depend on the block copolymer composition, type of amine, method of mixing, and solvent composition. In contrast, the

PLL-PAH/cit aggregates have phase-separation features on the order of hundreds of nanometers, and the phase-separation process involves only water; there is no organic cosolvent. The PLL-PAH phase separation does not involve oil-in-water emulsions either, in which oil droplets phase-separate from water. No oil is used in our synthesis. Interestingly, oil-in-water emulsions can be stabilized by particles as Pickering emulsions, forming capsular materials after cross-linking of the particles (39−41).

To ensure that this phase-separated two-polymer structure was not an artifact of dye conjugation, we performed the same experiment using non-dye-conjugated PLL and PAH. Differential interference contrast (42) microscopy indicated that the resulting aggregates also had similar internal structures (Figure 1c). These PLL-PAH/cit aggregates attached to the glass slide surface through charge attraction, which induced some spreading as observed previously for PLL/cit and PAH/cit aggregates (29). Though the surface-bound PLL-PAH/cit aggregates may not have had an internal structure identical with freely suspended ones, phase separation of the two different polyamines clearly occurred.

Adding the silicic acid solution to the above PLL-PAH/cit aggregate suspension yielded micron-sized solid particles similar to those previously reported (30), with the notable difference being that PAH was found as discrete submicron-sized domains surrounded by a continuous PLL domain (Figure 1d). This PAH-PLL spatial distribution indicates that silicic acid preserved the phase-separated bipolymer structure of the PAH-PLL/salt aggregates of Figure 1b. SEM analysis showed that these dried particles had protrusions on the surface (Figure 1e). It is difficult to say if they emerged during SEM sample preparations (during which the particles are dried) or if these protrusions exist on the solid particles under wet conditions (due to optical imaging limitations).
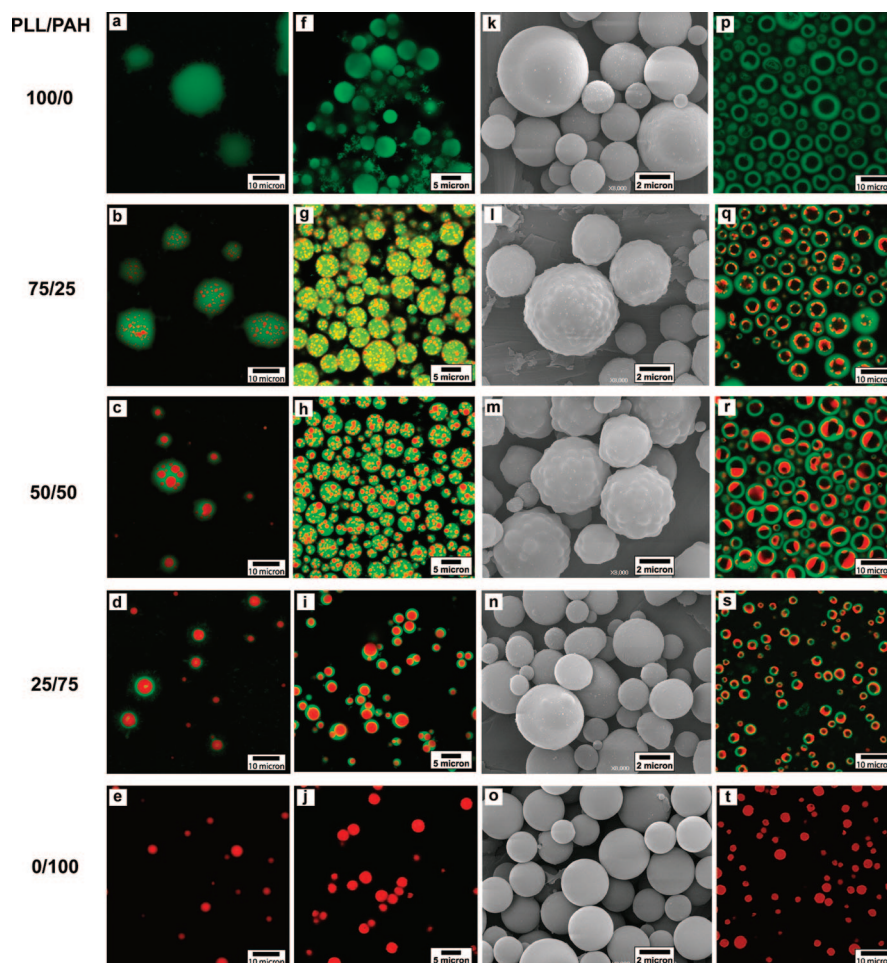
FIGURE 2. (a−e) Confocal microscopy images of PLL-PAH/cit aggregates synthesized at $R = 4$ and aged for 30 min. (f−j) Confocal microscopy and (k−o) SEM images of solid microspheres after the addition of silicic acid. (p−t) Confocal microscopy images of hollow microspheres after the addition of SiO$_2$ NPs.

These protrusions measured 200−700 nm at their base, close to the size range of the PAH domains of Figure 1d, and are not observed in spheres prepared with either PAH or PLL. We suggest that these protrusions are silica and PAH in composition.

When SiO$_2$ NPs were used in place of silicic acid, the resulting particles were found to be hollow, as expected. The PAH-PLL spatial distribution was markedly different, however. PLL was found as a continuous layer that marked the location of the silica/polymer shell wall (Figure 1f). In contrast, PAH was not found within the PLL layer, but rather it was found as discrete domains attached to the inner shell wall of the hollow capsules. These PAH domains are larger than the ones visualized inside the silicic-acid-derived solid spheres. Following our model for NP assembly of hollow spheres (29, 30), we suggest that the SiO$_2$ NPs diffuse and deposit on the PAH-PLL/cit aggregate in such a way that PLL is pulled outward toward the periphery by the NPs, forming the PLL/silica shell wall. During this process, the initially small PAH domains do not pull toward the periphery but, instead, coalesce onto the inner shell wall.

We studied the effect of the PLL-PAH ratio from 100:0 to 0:100 on the internal structure of the polymer/salt aggregates (Figure 2a−e). This ratio was changed using ap-

propriate PLL and PAH amounts while keeping the charge ratio R at 4. The PLL-PAH/cit aggregates formed at all ratios, showing a systematic change as the PLL-PAH ratio was varied. Individual PAH/cit and PLL/cit aggregates were not found.

PLL-PAH/cit aggregates showed an increasing volume amount of PAH domains with increasing PAH content. The numerous, small PAH domains seemed to coalesce into larger domains such that one polymer/salt aggregate was observed to be a single PAH domain covered by a PLL shell, at the PLL-PAH ratio of 25:75. Under PAH-rich conditions, isolated speckles of PLL could be seen within some PAH cores (Figure 2d). At all ratios, PAH was always found as discrete globules inside a contiguous PLL domain.

This phase-separated polymer structure was replicated in the resultant microspheres at all ratios also, after the addition of silicic acid (Figure 2f−j). A slight amount of homogenization of PLL and PAH was observed as a yellowish tinge in the confocal overlay images, which was most apparent at a PLL-PAH ratio of 75:25 (Figure 2g). This indicated partial remixing of PLL and PAH after silicic acid addition to form the silica/polymer microspheres. SEM analysis provided additional support for the correlation between the surface
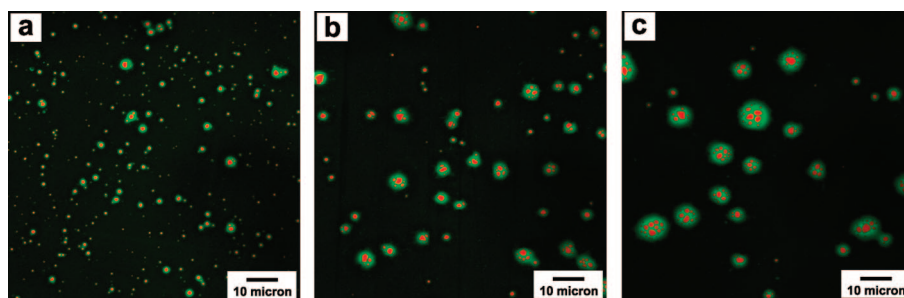
FIGURE 3. Confocal microscopy images of PLL-PAH (50:50)/cit aggregates aged for (a) 5 s, (b) 5 min, and (c) 30 min.
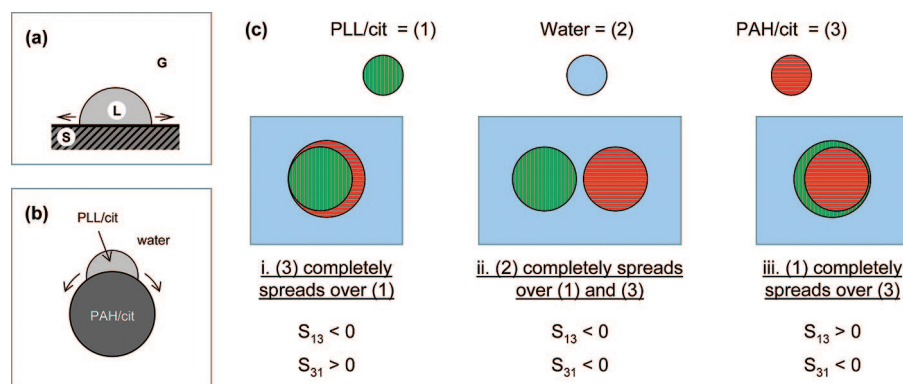

FIGURE 4. Schematics of (a) a liquid droplet spreading on a solid and (b) a PLL/cit domain spreading on a PAH/cit domain. (c) Possible equilibrium configurations when two immiscible liquid droplets come in contact within a third mutually immiscible liquid.

bumpiness and PAH domains; i.e., PAH domains lead to the presence of surface protrusions (Figure 2k–o).

The different PLL-PAH ratios led to hollow spheres with fascinating polymer spatial distributions (Figure 2p–t). PLL-only and PAH-only aggregates led to water-filled hollow spheres and polymer-filled hollow spheres, respectively, as mentioned earlier. PLL was localized in the shell wall, whereas PAH was localized in the shell wall and in the hollow spheres of the particle. The term "hollow", as should be reminded, indicates the capsular shell-like nature of the spherical particles (Scheme 1) (29, 30). The PLL-only hollow spheres were generally larger in diameter and fewer in number compared to the PAH-only hollow spheres, resulting from the larger but fewer PLL/cit aggregates compared to the PAH/cit aggregates (Figure 2a,e).

The use of both polyamines led to water-filled hollow spheres with PLL/silica shells and PAH domains mostly located on the inner shell wall (Figure 2q–s). With decreasing PLL-PAH ratio, the PAH domains increased in size and decreased in number as a likely result of coalescence. This was apparent when comparing materials prepared at PLL-PAH ratios of 75:25 and 50:50, where one could observe only one or two PAH domains in the latter and two or more domains in the former (Figure 2q,r). In the 25:75 case, the addition of SiO_2 NPs led to smaller hollow spheres in which both PLL and PAH localized in the shell wall. PAH domains were attached along the inner wall and, in many cases, were embedded in the shell wall (Figure 2s). This contrasted the large single or double PAH spherical domains situated eccentrically within the solid spheres (Figure 2l).

The key step in the formation of patchy hollow and solid spheres (with PAH domains located at the particle surface)

is the apparent phase separation of PAH/salt aggregates within the larger PLL/salt aggregates. To interpret this phenomenon in the context of earlier work that indicated that polymer/salt aggregates grew through coalescence (29, 30), we prepared a PLL-PAH/cit suspension and analyzed aliquots at different times (Figure 3). A total of 5 s after the 10-s gentle mixing of the polyamines and salt solutions, the aggregates essentially took on a PAH-core/PLL-shell structure (Figure 3a). A total of 5 min of growth time led to rapid increases in the average aggregate size and the amount of aggregates containing multiple PAH domains (Figure 3b), with the trend continuing for longer times (Figure 3c). Aging the PLL-PAH/cit aggregate suspension for too long (>1 h) resulted in a thin film at the bottom of the reaction tube. So, for the PLL-PAH/cit system, there seem to be two modes of coalescence: coalescence between PLL-PAH/cit aggregates and coalescence between the smaller PAH/cit domains inside a PLL-PAH/cit aggregate (Figure 3).

To explain how an aqueous solution of PLL and PAH undergoes polyamine separation in the presence of citrate anions, we extend our polymer/salt aggregation model from one polymer to two polymers. We propose that PLL and PAH electrostatically cross-link with citrate to form PLL/cit and PAH/cit aggregates, respectively, at initial contact in solution (nucleation stage; Figure S1 in the Supporting Information) These aggregates then interact via coalescence through up to three different pairwise combinations (i.e., PLL/cit + PLL/cit, PAH/cit + PAH/cit, and PLL/cit + PAH/cit) to form the PLL-PAH/cit aggregates (growth stage). If this case were true, then combining a PLL/cit suspension with a PAH/cit suspension would yield similarly mixed PLL-PAH/cit aggregates in

suspension, which was what we observed (Figure S2 in the Supporting Information).

The complex polymer structure of the PLL-PAH/cit aggregates (and the resulting silicic-acid-prepared microspheres) could be understood by considering that the morphologies result from the spreading of one phase (PLL/cit domains) over the other (PAH/cit domains) in water. For a liquid (L) drop on a solid surface (S) in a gas medium (G), spreading can be predicted by Harkin's equation, $S_{LS} = \gamma_{SG} - \gamma_{LG} - \gamma_{SL}$, where S_{LS} is the spreading coefficient, γ_{SG} and γ_{LG} are the surface tensions for the solid and liquid, respectively, and γ_{SL} is the solid/liquid interfacial tension (Figure 4a) (43). The drop is said to spread for positive S_{LS} values. Thus, for a PLL/cit domain to spread over a PAH/cit domain in water, $S_{PLL/cit-PAH/cit} = \gamma_{PAH/cit-water} - \gamma_{PLL/cit-water} - \gamma_{PLL/cit-PAH/cit} > 0$ (Figure 4b).

Following the approach by Hobbs et al. (44) and others for immiscible ternary polymer blends (42, 45, 46), we consider three simple structures that result from one PLL/cit aggregate ("1") and one PAH/cit aggregate ("3") suspended in water ("2") (Figure 4c). Case iii adequately describes the confocal image data for PLL-PAH/cit aggregates. The PAH/cit domains are always interior to the PLL/cit domains, which means that PLL/cit spreads completely over the PAH/cit aggregate, or $S_{13} = \gamma_{32} - \gamma_{12} - \gamma_{13} > 0$. This also means that PAH/cit does not spread over PLL/cit, or $S_{31} = \gamma_{12} - \gamma_{32} - \gamma_{31} < 0$. The condition of $\gamma_{32} > \gamma_{12}$ is readily derived, indicating that the higher surface tension of PAH/cit domains is responsible for PAH/cit domains being enveloped by PLL/cit. Adjusting the relative surface tension then may provide a means to controlling multicompartment formation in the eventual particles.

In summary, we report a new method to synthesize patchy, multicompartment organic/inorganic microspheres, which combines NP/polymer tandem assembly and polyamine demixing. The processing involves the room-temperature mixing of a PLL/PAH solution, a multivalent anion solution, and a silica source in sequence. The key observation was the PLL/PAH solution phase separating into a suspension of polymer/salt aggregates that contain heterogeneously mixed PLL and PAH domains. Coalescence reasonably explained the growth of the PLL-PAH/cit aggregates and of the PAH/cit domains inside the aggregates, and surface tension differences explained the presence of PAH/cit domains within PLL/cit domains. Silicic acid preserved the general shape and size of these aggregates in the form of solid microspheres; PAH was found in discrete domains throughout the solid spheres. Silica NPs led to the formation of water-filled hollow microspheres, in which PAH/cit domains were found attached to the inner shell wall. Under high-PAH-ratio conditions, PAH was found at the particle surface as patches. Work is ongoing to control surface patchiness and compartmentalization of these anisotropic silica/polyamine microparticles for targeted delivery and triggered chemical release applications and to study the use of other polyamines and NP compositions.

Supporting Information Available: Schematic for the proposed formation mechanism of microphase-separated polyamine aggregates (Figure S1) and images of aged PLL-PAH/cit aggregates (Figure S2). This material is available free of charge via the Internet at http://pubs.acs.org.

REFERENCES AND NOTES

(1) Glotzer, S. C.; Solomon, M. J. *Nat. Mater.* **2007**, *6*, 557–562.
(2) Yoshida, M.; Lahann, J. *ACS Nano* **2008**, *2*, 1101–1107.
(3) Zhang, Z.; Keys, A. S.; Chen, T.; Glotzer, S. C. *Langmuir* **2005**, *21*, 11547–11551.
(4) Zhang, Z.; Glotzer, S. *Nano Lett.* **2004**, *4*, 1407–1413.
(5) Yin, Y.; Alivisatos, A. P. *Nature* **2005**, *437*, 664–670.
(6) Nelson, D. R. *Nano Lett.* **2002**, *2*, 1125–1129.
(7) Min, Y. J.; Akbulut, M.; Kristiansen, K.; Golan, Y.; Israelachvili, J. *Nano Lett.* **2008**, *7*, 527–538.
(8) Glotzer, S. *Science* **2004**, *306*, 419–420.
(9) Takei, H.; Shimuzu, N. *Langmuir* **1997**, *13*, 1865–1868.
(10) Nakahama, K.; Kawaguchi, H.; Fujimoto, K. *Langmuir* **2000**, *16*, 7882–7886.
(11) Lu, Y.; Xiong, H.; Jiang, X.; Xia, Y.; Prentiss, M.; Whitesides, G. *J. Am. Chem. Soc.* **2003**, *125*, 12724–12725.
(12) Cayre, O.; Paunov, V.; Velev, O. *J. Mater. Chem.* **2003**, *13*, 2445–2450.
(13) Yaseen, M. A.; Yu, J.; Wong, M. S.; Anvari, B. *Biotechnol. Prog.* **2007**, *23*, 1431–1440.
(14) Choi, J.; Zhao, Y.; Zhang, D.; Chien, S.; Lo, Y. *Nano Lett.* **2003**, *3*, 995–1000.
(15) Love, J.; Gates, B.; Wolfe, D.; Paul, K.; Whitesides, G. *Nano Lett.* **2002**, *2*, 891–894.
(16) Petit, L.; Manaud, J.; Mongotaud, C.; Ravaine, S.; Duguet, E. *Mater. Lett.* **2001**, *51*, 478–484.
(17) Jackson, A. M.; Myerson, J. W.; Stellacci, F. *Nat. Mater.* **2004**, *3*, 330–336.
(18) Burda, C.; Chen, X. B.; Narayanan, R.; El-Sayed, M. A. *Chem. Rev.* **2005**, *105*, 1025–1102.
(19) Li, Z. B.; Kesselman, E.; Talmon, Y.; Hillmyer, M. A.; Lodge, T. P. *Science* **2004**, *306*, 98–101.
(20) Perro, A.; Reculusa, S.; Ravaine, S.; Bourgeat-Lami, E. B.; Duguet, E. *J. Mater. Chem.* **2005**, *15*, 3745–3760.
(21) Yang, S. M.; Kim, S. H.; Lim, J. M.; Yi, G. R. *J. Mater. Chem.* **2008**, *18*, 2177–2190.
(22) Chen, H. Y.; Zhao, Y.; Song, Y. L.; Jiang, L. *J. Am. Chem. Soc.* **2008**, *130*, 7800–7801.
(23) Roh, K. H.; Martin, D. C.; Lahann, J. *J. Am. Chem. Soc.* **2006**, *128*, 6796–6797.
(24) Utada, A. S.; Lorenceau, E.; Link, D. R.; Kaplan, P. D.; Stone, H. A.; Weitz, D. A. *Science* **2005**, *308*, 537.
(25) Wan, J.; Bick, A.; Sullivan, M.; Stone, H. A. *Adv. Mater.* **2008**, *20*, 3314–3318.
(26) Kubowicz, S.; Baussard, J. F.; Lutz, J. F.; Thunemann, A. F.; von Berlepsch, H.; Laschewsky, A. *Angew. Chem., Int. Ed.* **2005**, *44*, 5262–5265.
(27) Cui, H. G.; Chen, Z. Y.; Zhong, S.; Wooley, K. L.; Pochan, D. J. *Science* **2007**, *317*, 647–650.
(28) Murthy, V. S.; Cha, J. N.; Stucky, G. D.; Wong, M. S. *J. Am. Chem. Soc.* **2004**, *126*, 5292–5299.
(29) Murthy, V. S.; Rana, R. K.; Wong, M. S. *J. Phys. Chem. B* **2006**, *110*, 25619–25627.
(30) Rana, R. K.; Murthy, V. S.; Yu, J.; Wong, M. S. *Adv. Mater.* **2005**, *17*, 1145–1150.
(31) Yu, J.; Murthy, V. S.; Rana, R. K.; Wong, M. S. *Chem. Commun.* **2006**, 1097–1099.
(32) Yu, J.; Yaseen, M. A.; Anvari, B.; Wong, M. S. *Chem. Mater.* **2007**, *19*, 1277–1284.
(33) Kadali, S. B.; Soultanidis, N.; Wong, M. S. *Top. Catal.* **2008**, *49*, 251–258.
(34) Caruso, F. *Chem.—Eur. J.* **2000**, *6*, 413–419.

(35) Donath, E.; Sukhorukov, G. B.; Caruso, F.; Davis, S. A.; Mohwald, H. *Angew. Chem., Int. Ed.* **1998**, *37*, 2202–2205.

(36) Pochan, D. J.; Chen, Z. Y.; Cui, H. G.; Hales, K.; Qi, K.; Wooley, K. L. *Science* **2004**, *306*, 94–97.

(37) Hales, K.; Chen, Z. Y.; Wooley, K. L.; Pochan, D. J. *Nano Lett.* **2008**, *8*, 2023–2026.

(38) Cui, H. G.; Chen, Z. Y.; Wooley, K. L.; Pochan, D. J. *Macromolecules* **2006**, *39*, 6599–6607.

(39) Dinsmore, A. D.; Hsu, M. F.; Nikolaides, M. G.; Marquez, M.; Bausch, A. R.; Weitz, D. A. *Science* **2002**, *298*, 1006–1009.

(40) Binks, B. P. *Curr. Opin. Colloid Interface Sci.* **2002**, *7*, 21–41.

(41) Hsu, M. F.; Nikolaides, M. G.; Dinsmore, A. D.; Bausch, A. R.; Gordon, V. D.; Chen, X.; Hutchinson, J. W.; Weitz, D. A. *Langmuir*

(42) Guo, H. F.; Packirisampy, S.; Gvozdic, N. V.; Meier, D. J. *Polymer* **1997**, *38*, 785–794.

(43) Harkins, W. D. *The Physical Chemistry of Surface Films*; Reinhold Publishing Co.: New York, 1952.

(44) Hobbs, S. Y.; Dekkers, M. E. J.; Watkins, V. H. *Polymer* **1988**, *29*, 1598.

(45) Legros, A.; Favis, B. D.; Carreau, P.; Michel, A. *Polymer* **1997**, *38*, 5085–5089.

(46) Reignier, J.; Favis, B. D. *Macromolecules* **2000**, *33*, 6998–7008.

2005, *21*, 2963–2970.